Three-Terminal Single-Molecule Junctions Formed by Mechanically Controllable Break Junctions with Side Gating

Dong Xiang,[†,‡] Hyunhak Jeong,[†] Dongku Kim,[†] Takhee Lee,*[,†] Yongjin Cheng,[‡] Qingling Wang,[§] and Dirk Mayer*[,‖]

[†]Department of Physics and Astronomy, Seoul National University, Seoul 151-747, Korea

[‡]School of Mathematics and Physics, China University of Geosciences, Wuhan 430074, China

[§]Faculty of Mechanical and Electronic Information, China University of Geosciences, Wuhan 430074, China

[‖]Peter-Grünberg-Institute, PGI-8, Research Center Jülich and JARA Fundamentals of Future Information Technology, Jülich 52425, Germany

S Supporting Information

ABSTRACT: Molecules are promising candidates for electronic device components because of their small size, chemical tunability, and ability to self-assemble. A major challenge when building molecule-based electronic devices is forming reliable molecular junctions and controlling the electrical current through the junctions. Here, we report a three-terminal junction that combines both the ability to form a stable single-molecule junction via the mechanically controllable break junction (MCBJ) technique and the ability to shift the energy levels of the molecule by gating. Using a noncontact side-gate electrode located a few nanometers away from the molecular junction, the conductance of the molecule could be dramatically modulated because the electrical field applied to the molecular junction from the side gate changed the molecular electronic structure, as confirmed by the ab initio calculations. Our study will provide a new design for mechanically stable single-molecule transistor junctions fabricated by the MCBJ method.

KEYWORDS: Molecular electronics, electron transport, molecular transistors, single molecule junction, mechanically controllable break junction, nanogap electrodes
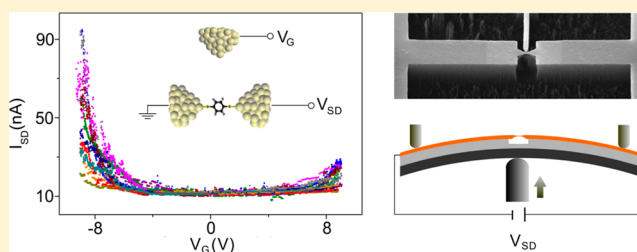
Producing molecular electronic devices in which individual molecules or molecular monolayers are utilized as active electronic components is a promising approach for the ultimate miniaturization and integration of electronic devices.[1−5] In particular, building a single-molecule field-effect transistor (FET) is considered a critical step in molecular electronics. Although previous theoretical calculations have demonstrated that single molecules can be used as an active channel in FETs,[6−12] an experimental demonstration of a true three-terminal device, one that depends on external modulation of molecular orbitals, has been a tremendous challenge because it requires one to (1) find a reliable method to bridge a single molecule to the source and drain electrodes and (2) place the gate electrode a few nanometers away from the molecule to achieve the required gate field.[13]

Previous efforts to overcome these challenges have coupled an electrochemical gate electrode[13−16] or a bottom-gate electrode into a molecular junction.[17−28] The electrochemical gate can effectively control the current through the molecules,[13−15] but it can only be operated in electrolytes. The bottom gate can directly modulate the molecular orbital electrostatically in a molecular FET contact configuration. However, it is not trivial to obtain stable and high-yield single-molecule junctions with the bottom-gate configuration.[23]

Motivated by the bottom-gate design, we adopted a three-terminal device that combines both the ability to form a mechanically stable single-molecule junction and the ability to shift the energy levels of the molecule using a side-gate electrode in a noncontact configuration.[29,30] Our experiments, supported by first-principle calculations, demonstrate that the properties of electronic transport through the single-molecule junction can be directly modulated by the external electrical field of the side gate and will enhance the prospects for three-terminal molecular electronic devices.

The scheme for combining electrostatic gating and mechanical adjustability is to add a gate electrode to a mechanically controlled break junction (MCBJ), as shown in Figure 1a. The MCBJ technique has been widely used to study electronic transport in molecular electronics, and many significant results have been obtained.[31−43] Spring steel substrates were used for the fabrication of the MCBJ chips. Electrode structures containing a thin bridge with a constriction of 30 nm and a nanoscale side-gate electrode were defined by e-beam lithography (Figure 1b). After the lift-off of a 40 nm thick

ACS Publications © XXXX American Chemical Society

A

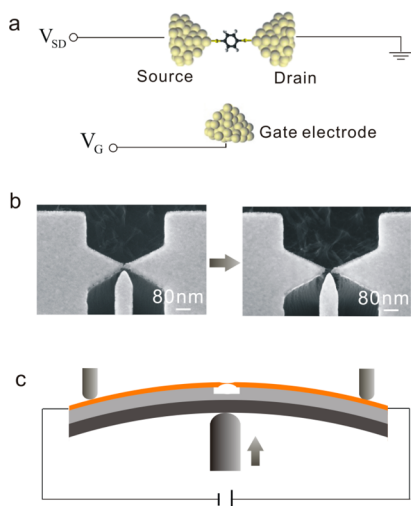dx.doi.org/10.1021/nl401067x | Nano Lett. XXXX, XXX, XXX−XXX

Figure 1. (a) Schematic illustrating a molecular transistor junction. An external electric field generated by a side-gate electrode is applied to the single-molecule junction formed by the MCBJ. Note that the distance (∼5 nm) from gate to molecular junction for working molecular transistor junctions is not scaled proportionally in this schematic. (b) Top view of a scanning electron microscopy (SEM) image of a microfabricated MCBJ chip consisting of a freestanding metal bridge with a gate electrode (left SEM image). The push rod exerts a bending force to bend the substrate and breaks the metal bridge at the smallest constriction, resulting in two separated electrodes (right SEM image). (c) Schematic of the MCBJ setup. The distance between the electrodes for both opening and closing operation modes can be tuned by bending or relaxing the substrate, respectively.

Au film, the isolating layer was locally removed by reactive ion etching to generate a suspended metal bridge[34,44,45] (see Figure S1 in the Supporting Information for detailed information about the chip fabrication).

The fabricated chip was mounted into a homemade three-point bending apparatus. The two outer posts of the three-point bending apparatus were fixed, while the third one worked as a push rod in the Z direction, as shown in Figure 1c. When the push rod exerts a bending force on the substrate, the movement in the Z direction causes an elongation of the constriction until the bridge breaks, resulting in two separated electrodes that act as source and drain electrodes. The distance between the source and drain electrodes for both the opening and the closing operation modes was tuned by bending or relaxing the substrate, respectively (see Figure S3 in the Supporting Information). The precision of the gap between two electrodes is determined by the attenuation factor. For our setup, the gap can be controlled, in principle, with sub-Angstrom accuracy[44−46] (see Figures S4 and S5 in the Supporting Information).

The 1,4-benzenedithiol (denoted as BDT), a conjugated molecule with two thiol termini as binding groups, was integrated between the two electrodes to form a metal/molecule/metal junction. For this purpose, a 1 mM ethanol solution of BDT was prepared in a protective atmosphere in which the oxygen level was less than 1 ppm. After a self-assembly period of 10 min on the Au surface, the sample was thoroughly rinsed with ethanol and dried in a nitrogen stream. Subsequently, the samples were mounted into the MCBJ. The gate-effected conductance measurement was performed at room temperature.

The breaking process of the metal bridge with assembled molecules on the surface was investigated. A state can be identified in which two electrodes become bridged by a single molecule by monitoring the conductance change during the junction-breaking process (Figure 2). First, the breaking
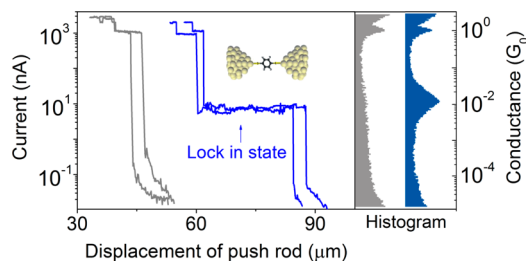

Figure 2. Tunneling currents as a function of the push rod displacement in the open gap period. In the case of the BDT molecular junction (blue curves), the current jumped to a plateau (lock-in state) during the open period. In the lock-in state, the current was almost independent of the gap size, indicating a metal/molecule/metal junction was formed (cartoon). In contrast, the lock-in state was absent in the molecule-free junction (gray curve). A bias voltage of 12 mV was applied between the source and drain electrodes. The current histogram extracted from 200 curves indicates that there is a peak for the lock-in state in the molecular junction, whereas no such peak exists in molecule-free junctions.

process of the metal wire is observed, which causes discrete conductance values of multiples of G_o (G_o, the conductance quantum, $7.75 \times 10^{-5} \, \Omega^{-1}$). The molecule can bind covalently to both the electrodes of the MCBJ by the two thiol termini of BDT, and a metal/molecule/metal junction is formed. In particular, typical plateaus, which correspond to a lock-in state, were always observed in the molecular junction after the breaking of the metal bridge. During such a lock-in state, the conductance of the molecular junction was almost independent of the displacement of the push rod. Normally, the last plateau of the current before the junction completely collapses is attributed to a single metal/molecule/metal junction. More than 200 metal/molecule/metal junctions were analyzed, and the single-molecule conductance was determined statistically to be $1.1 \times 10^{-2} \, G_o$, which is consistent with previous reports.[47−49] Compared with the molecular junctions, no pronounced plateau was observed at values below 1 G_o in the junctions without molecules, as shown in Figure 2.

The conductance of molecular junction at different gate voltages was subsequently analyzed by a statistical method. Figure 3 shows the corresponding histograms at different gate voltages. It can be seen from this figure that the typical peaks did not obviously shift at different gate voltage. However the peaks were broadened to a higher conductance value as the gate voltage increased negatively. The broad peaks can be attributed to the variation of effective gate coupling (i.e., depending on the exact molecule position with respect to the side gate electrode).

Once a metal/molecule/metal junction was constructed, the source and drain electrodes were frozen, and the current through two electrodes in the molecular junction (I_{sd}) was recorded with a fixed bias voltage (12 mV) while sweeping the gate voltage V_G.

The gate-controlled current as a function of gate voltage is illustrated in Figure 4a. The tunnel current passing through the molecular junction was weakly dependent on the gate voltage
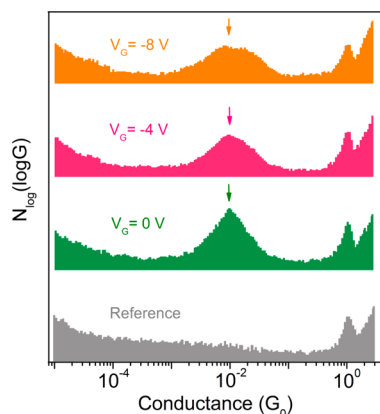
Figure 3. Conductance histograms at different gate voltages. The bottom histogram is the reference histogram from molecule-free junctions and other histograms are those for molecular junctions at different gate voltages of 0, −4, and −8 V. Each histogram was built from 200 conductance curves obtained during the open cycle process. The arrow in each histogram indicates the conductance peak. The source−drain voltage was fixed at 12 mV.
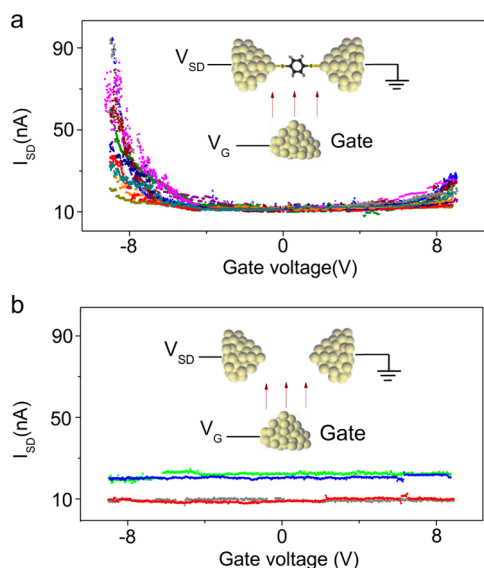

Figure 4. Source−drain current (I_{SD}) versus gate voltage (V_G) curves for the Au-BDT-Au molecular and molecule free three-terminal junction. (a) The current was modulated by the gate voltage in 12 different molecular junctions. (b) No gate-controlled current was observed in the molecule-free junction (red and gray curves). When the gap size between the source and drain electrodes was reduced by ∼0.1 nm, the tunneling current increased slightly, but no gate-effected current was observed (green and blue curves). The inset schematics illustrate the three-terminal junction (a) with or (b) without BDT bridged between the source and drain electrodes.

for bias voltages within ±3 V. However, the current and corresponding conductance value increased rapidly as the gate voltage became more negative. The effective gate effect is attributed to the special geometry of the electrodes. Since a pair of taped source−drain electrodes will be formed naturally during the break of metal bridge in our experiments. An independent simulation demonstrated that nonuniform tapered electrodes can yield 3 orders of magnitude improvement in gate coupling compared to the case of the uniform (rectangular) bulk electrodes.[50] It should be noted that the molecular junctions became unstable, even collapsing, when the applied

gate voltage increased beyond ±10 V. Therefore, we could only record the current at either high positive or high negative bias voltages in one measurement. In cases in which the metal/molecule/metal junction is broken, the molecular junctions can be rebuild (with ∼50% yield) by decreasing the gap size between two electrodes by 0.2−0.4 nm followed by withdrawing the electrodes to the same gap size as before. Then, the gate-modulated current can be observed again after the single-molecule junction is reformed. In this sense, there are certainly advantages in MCBJ-type molecular transistor junctions compared to other kind of junctions, such as electromigration fabricated nanogap junctions.

Three types of chips were investigated, and the gate electrode was located in various positions relative to the axis between the source and drain electrodes (see Figure S2 in the Supporting Information). More than 100 individual molecular junctions within the three types of chips were examined. We found that only those chips for which the gate electrode was close enough to the molecular junction (the perpendicular distance from the gate electrode to the tip axis was less than 10 nm) displayed typical FET behavior. For these chips, 12 out of 67 junctions showed typical FET behavior (∼18% yield), as shown in Figure 4a and Table S1. Please note that the gate efficiency is sensitive to the exact position of molecules with respect to the side gate. For those molecules located far away from the side facing the gate, the screening of the gold electrodes will be dominant which results in the failure of FET behavior. Even for those junctions that exhibited FET behavior, the gated tunneling current spread over a wide range especially under the negative gate voltage, which agrees with the observation shown in Figure 3. The variation of the gate coupling from junction to junction becomes clearer when we plot the modulation ratio of each junction, as shown in Figure S10 in the Supporting Information. Interestingly, for all the FET behavior junctions, the increase of the current at negative gate voltages is larger than for positive gate voltages, resulting in an asymmetric I_{SD} versus V_G.

In contrast to the molecular junction, no gate effect current was observed when the molecules were absent (called as molecule-free junction) even at different gap sizes (Figure 3b). Four different types of molecule-free junctions were tested, in which the relative positions of the source and drain electrodes were dramatically changed: the first configuration involved direct point-to-point contact of bare Au atoms between the source and drain electrode in which the corresponding conductance was observed to be 1 G_o, and the remaining configurations involved changing the relative distance between the source and drain electrode to be smaller than, equal to, and larger than 1 nm (approximate BDT molecule length). Note that the current was almost independent of the gate voltage in all four types of molecule-free junctions (see Figure S6 in the Supporting Information). By comparing the results of Figures 4 and Figure S6, it can be concluded that the observed variation of the current was caused by the modulation of the electronic structure of the molecules by the applied gate voltage. It should be noted that leakage current level is important for molecular transistors. We measured the gate−source current (I_{GS}) and gate−drain (I_{GD}) current at different gate voltages. We found that the leakage current was almost 3 orders of magnitude smaller than the current passing through the molecular junction and it was almost close to the limitation of the measurement setup (see Figure S7 in the Supporting Information).

C

dx.doi.org/10.1021/nl401067x | Nano Lett. XXXX, XXX, XXX−XXX

To further clarify how the electronic transport was affected by the gate electrode, first-principle calculations based on density functional theory (DFT) with the Dmol3 simulation package were performed to explore the electronic transport properties.[6−9,51] Before this step, determination of the value of the electric field strength and potential around the molecular junction is necessary. Here, the simulation of the electrical field and the potential distribution was carried out with COMSOL Multiphysics using an electrostatic physics model. The geometry of the three electrodes was assumed to be a cone-like body with a sphere-like tip. The gap size between the source and drain electrodes was 1.1 nm, the molecule length. The perpendicular distance between the gate electrode and the source−drain axis was set to 5 nm, while different voltages were applied to the gate electrode. From the simulation, we found that the electrical field strength between the source and drain electrodes with a gate bias is an order of magnitude larger than that for the case when the gate electrode was absent (see Figure S8 in the Supporting Information). Our simulation also showed that the field distribution as well as the potential distribution around the gate electrode was inhomogeneous and that it strongly depended on the location of the gate electrode with respect to the source and drain electrodes, as shown in Figure 5a and Figure S9. We fixed the position of the gate electrode in the center between the source and drain electrodes and extracted the average value of the electric field from the simulation. This value was used as input for the following DFT calculation.

The local density approximation (LDA) with PWC (Perdew−Wang approaches for the correlation functional) was used to describe the exchange-correction energy functional. The numerical basis set of DNP (double numerical plus polarization) was adopted. In our calculations, the cutoff energy, which determines the number of plane-wave basis functions, is chosen to be 380 eV. In our model for DFT calculation, the molecule contacted the source and drain electrodes through S−Au bonding with two different configurations (in-plane and out-of-plane configurations) to form an Au/1,4-BDT/Au junction. The DFT calculations showed that the wave function density of the molecular orbital varied tremendously at different gate voltages in both configurations. Figure 5b shows the in-plane configuration case in which the bonding Au atom is located parallel to the benzene ring plane. When the electric field was gradually increased, the delocalization of the HOMO (highest occupied molecular orbital) increased as well. The HOMO for $V_G = -9$ V became more delocalized than that for $V_G = 0$ V. For the out-of-plane configuration in which the bonding Au atom deviates from the benzene ring plane, a significant variation of the molecular orbitals was predicted when an electrical field was applied (see Figure S11 in the Supporting Information). The DFT calculation results indicated that the electronic structure of the molecular junction was dramatically changed at a higher electric field, which is qualitatively consistent with our experimental data.

In summary, we studied three-terminal transistor single-molecular junctions formed by the mechanically controlled break junction (MCBJ) technique with a noncontact side gate. The distance between the source and drain electrodes was precisely controlled to achieve a single-molecule junction, while an in-plane gate-electrode was coupled into the molecular junction to shift the molecular energy levels. Our experimental results combined with the DFT calculations demonstrated that
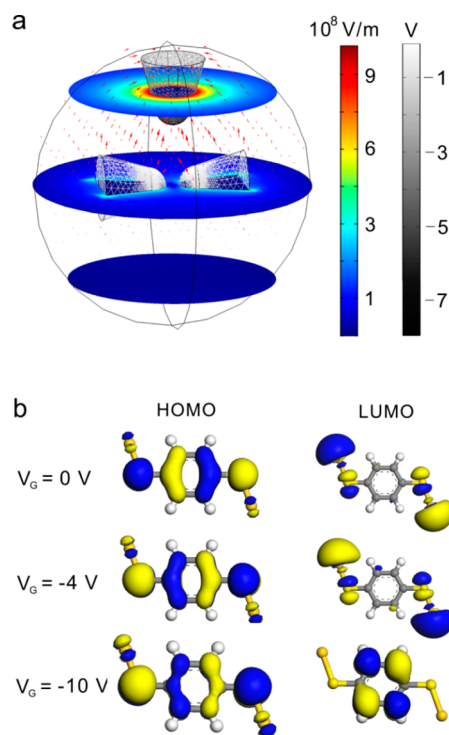

Figure 5. (a) Simulation results of the electrical field distribution with the gate voltage of −8 V and the source−drain voltage of 12 mV. The source and drain electrodes were separated by 1.1 nm, and the perpendicular distance between the gate and the source−drain axis was set to 5 nm. The arrows indicate the electrical field vector directions. Two color bars were used: one (left color bar) shows the electrical field strength distribution on three cross sections, and the other (right gray bar) presents the potential distribution on the electrode surface. (b) The gate voltage dependence of the spatial distribution of the HOMO and LUMO for an in-plane configuration in which the bonding Au atom is located parallel to the benzene ring plane. Blue and yellow regions indicate regions with positive and negative wave function amplitudes, respectively. With increasing gate voltages, both the HOMO and LUMO tend to become delocalized.

direct modulation of the electronic transport characteristics through a single-molecule junction with side gating was possible, yielding a new design platform for mechanically stable single-molecule transistor junctions.

■ ASSOCIATED CONTENT

Ⓢ Supporting Information
Chip fabrication, experimental setup, calculation of the attention factor, characterization of molecule-free junctions, simulation of the electrical field, and three terminal molecular transistor junctions. This material is available free of charge via the Internet at http://pubs.acs.org.

■ AUTHOR INFORMATION

Corresponding Author
*E-mail: tlee@snu.ac.kr (T.L.); dirk.mayer@fz-juelich.de (D.M.).

Notes
The authors declare no competing financial interest.

■ ACKNOWLEDGMENTS

■ ABBREVIATIONS

MCBJ, mechanically controllable break junction; FET, field-effect transistor; BDT, benzenedithiol; HOMO, highest occupied molecular orbital; LUMO, lowest unoccupied molecular orbital; DFT, density functional theory

■ REFERENCES

(1) Cuevas, J. C; Scheer, E. *Molecular Electronics: An Introduction to Theory and Experiment*; World Scientific Publishing Co. Pte. Ltd.: Singapore, 2010; pp 12−45.

(2) Yoon, H. J.; et al. *Angew. Chem., Int. Ed.* **2012**, *124*, 4736−439.

(3) Reus, W. F.; Thuo, M. M.; Shapiro, N. D.; Nijhuis, C. A.; Whitesides, G. M. *ACS Nano* **2012**, *6*, 4806−4822.

(4) Kasper, M. P.; Bjørnholm, T. *Nat. Nanotechnol.* **2009**, *4*, 551−556.

(5) Joachim, C.; Gimzewski, J. K.; Aviram, A. *Nature* **2000**, *408*, 541−548.

(6) Liang, Y. Y.; Chen, H.; Mizuseki, H.; Kawazoe, Y. *J. Chem. Phys.* **2011**, *134*, 144113.

(7) Shimazaki, T.; Yamashita, K. *Nanotechnology* **2007**, *18*, 424012.

(8) Damle, P.; Rakshit, T.; Paulsson, M.; Datta, S. *Nanotechnology* **2002**, *1*, 145−153.

(9) Di Ventra, M.; Pantelides, S. T.; Lang, N. D. *Appl. Phys. Lett.* **2000**, *76*, 3448.

(10) Osorio, E. A.; Bjørnholm, T.; Lehn, J.-M.; Ruben, M.; van der Zant, H. S. *J. Phys.: Condens. Matter* **2008**, *20*, 374121.

(11) Xu, Y.; et al. *Appl. Phys. Lett.* **2011**, *99*, 043304.

(12) Ke, S. H.; Baranger, H. U.; Yang, W. *Phys. Rev. B* **2005**, *71*, 113401.

(13) Xu, B. Q.; Xiao, X. Y.; Yang, X. M.; Zhang, L.; Tao, N. *J. Am. Chem. Soc.* **2005**, *127*, 2386−2387.

(14) Tao, N. J. *J. Mater. Chem.* **2005**, *15*, 3260−3263.

(15) Grunder, S.; Huber, R.; Wu, S.; Schönenberger, C.; Calame, M.; Mayor, M. *Chimia* **2010**, *64*, 140−144.

(16) White, H. S.; Kittlesen, G. P.; Wrighton, M. S. *J. Am. Chem. Soc.* **1984**, *106*, 5375−5377.

(17) Keane, Z. K.; Ciszek, J. W.; Tour, J. M.; Natelson, D. *Nano Lett.* **2006**, *6*, 1518−1521.

(18) Ghosh, A. W.; Rakshit, T.; Datta, S. *Nano Lett.* **2004**, *4*, 565−568.

(19) Park, H.; Park, J.; Lim, A. K. L.; Anderson, E. H.; Alivisatos, A. P.; McEuen, P. L. *Nature* **2000**, *407*, 57−60.

(20) Martin, C. A.; van Ruitenbeek, J. M.; van der Zant, H. S. J. *Nanotechnology* **2010**, *21*, 265201.

(21) Champagne, A. R.; Pasupathy, A. N.; Ralph, D. C. *Nano Lett.* **2005**, *5*, 305−308.

(22) Liang, W.; Shores, M. P.; Bockrath, M.; Long, J. R.; Park, H. *Nature* **2002**, *417*, 725−729.

(23) Song, H.; et al. *Nature* **2009**, *462*, 1039−1043.

(24) Piva, P. G.; et al. *Nature* **2005**, *435*, 658−661.

(25) Kubatkln, S.; et al. *Nature* **2003**, *425*, 698−701.

(26) Visconti, P.; Torre, A. D.; Maruccio, G.; D'Amone, E.; Bramanti, A.; Cingolani, R.; Rinaldi, R. *Nanotechnology* **2004**, *14*, 807−811.

(27) Osorio, E. A.; et al. *Nano Lett.* **2007**, *7*, 3336−3342.

(28) Osorio, E. A.; Ruben, M.; Seldenthuis, J. S.; Lehn, J.; van der Zant, H. S. J. *Small* **2010**, *6*, 174−178.

(29) Mangin, A.; Anthore, A.; Della Rocca, M. L.; Boulat, E.; Lafarge., P. *J. Appl. Phys.* **2009**, *105*, 014313.

(30) Martin, C. A.; Smit, R. H. M.; van der Zant, H. S. J.; van Ruitenbeek, J. M. *Nano Lett.* **2009**, *9*, 2940−2945.

(31) Lörtscher, E.; Gotsmann, B.; Lee, Y.; Yu, L.; Rettner, C.; Riel, H. *ACS Nano* **2012**, *6*, 4931−4939.

(32) Wheeler, P. J.; Russom, J. N.; Evans, K.; King, N. S.; Natelson, D. *Nano Lett.* **2010**, *10*, 1287−1292.

(33) Kim, Y.; et al. *Nano Lett.* **2012**, *12*, 3736−3742.

(34) Wu, S.; et al. *Nat. Nanotechnol.* **2008**, *3*, 569−574.

(35) Lörtscher, E.; Weber, H. B.; Riel, H. *Phys. Rev. Lett.* **2007**, *98*, 176807.

(36) Parks, J. J.; et al. *Science* **2010**, *328*, 1370−1373.

(37) Diez-Perez, I.; et al. *Nat. Nanotechnol.* **2011**, *6*, 226−231.

(38) Reed, M. A.; et al. *Science* **1997**, *278*, 252−254.

(39) Smit, R. H. M.; et al. *Nature* **2002**, *419*, 906−909.

(40) Kim, Y.; Song, H.; Strigl, F.; Pernau, H.-F.; Lee, T.; Scheer, E. *Phys. Rev. Lett.* **2011**, *106*, 196804.

(41) Ballmann, S.; et al. *Phys. Rev. Lett.* **2012**, *109*, 056801.

(42) Tsutsui, M.; Taniguchi, M.; Kawai, T. *Nano Lett.* **2009**, *9*, 1659−1662.

(43) Tsutsui, M.; Taniguchi, M. *J. Appl. Phys.* **2013**, *113*, 084301.

(44) Xiang, D.; et al. *Chem.—Eur. J.* **2011**, *47*, 13166.

(45) Xiang, D.; Zhang, Y.; Pyatkov, F.; Offenhäusser, A.; Mayer, D. *Chem. Commun.* **2011**, *47*, 4760−4762.

(46) Zhou, C.; Muller, C. J.; Deshpande, M. R.; Sleight, J. W.; Reed, M. A. *Appl. Phys. Lett.* **1995**, *67*, 1160−1162.

(47) Tian, J.; et al. *Nanotechnology* **2010**, *21*, 274012.

(48) Xiao, X.; Xu, B.; Tao, N. J. *Nano Lett.* **2004**, *4*, 267−271.

(49) Kim, Y.; Pietsch, T.; Erbe, A.; Belzig, W.; Scheer, E. *Nano Lett.* **2011**, *11*, 3734−3738.

(50) Datta, S. S.; Strachan, D. R.; Charlie Johnson, A. T. *Phys. Rev. B* **2009**, *79*, 205404.

(51) Mishchenko, A.; et al. *J. Am. Chem. Soc.* **2011**, *133*, 184−187.